Since January 2020 Elsevier has created a COVID-19 resource centre with free information in English and Mandarin on the novel coronavirus COVID-19. The COVID-19 resource centre is hosted on Elsevier Connect, the company's public news and information website.

BBA - Molecular Basis of Disease 1868 (2022) 166289

Contents lists available at ScienceDirect

BBA - Molecular Basis of Disease

journal homepage: www.elsevier.com/locate/bbadis

Changes in glomerular filtration rate and metabolomic differences in severely ill coronavirus disease survivors 3 months after discharge

Mei Zhou [a,1], Xueyun Tan [a,1], Ping Luo [b,1], Juanjuan Xu [a,1], Zhengrong Yin [a], Tingting Liao [a], Sufei Wang [a], Zhihui Wang [c], Yang Jin [a,*]

[a] Department of Respiratory and Critical Care Medicine, NHC Key Laboratory of Pulmonary Diseases, Union Hospital, Tongji Medical College, Huazhong University of Science and Technology, 1277 Jiefang Rd, Wuhan, Hubei 430022, China
[b] Department of Translational Medicine Center, Union Hospital, Tongji Medical College, Huazhong University of Science and Technology, Wuhan, Hubei 430022, China
[c] Department of Scientific Research, Union Hospital, Tongji Medical College, Huazhong University of Science and Technology, Wuhan, Hubei 430022, China

ARTICLE INFO

Keywords:
Severely ill COVID-19 survivors
3 months after discharge
Renal outcome
Estimated glomerular filtration rate (eGFR)
Plasma metabolomic profiling

ABSTRACT

To explore the recovery of renal function in severely ill coronavirus disease (COVID-19) survivors and determine the plasma metabolomic profile of patients with different renal outcomes 3 months after discharge, we included 89 severe COVID-19 survivors who had been discharged from Wuhan Union Hospital for 3 months. All patients had no underlying kidney disease before admission. At patient recruitment, renal function assessment, laboratory examination, chest computed tomography (CT) were performed. Liquid chromatography–mass spectrometry was used to detect metabolites in the plasma. We analyzed the longitudinally change in the estimated glomerular filtration rate (eGFR) based on serum creatinine and cystatin-c levels using the CKD-EPI equation and explored the metabolomic differences in patients with different eGFR change patterns from hospitalization to 3 months after discharge. Lung CT showed good recovery; however, the median eGFR significantly decreased at the 3-month follow-up. Among the 89 severely ill COVID-19 patients, 69 (77.5%) showed abnormal eGFR (<90 mL/min per 1.73 m^2) at 3 months after discharge. Age (odds ratio [OR] = 1.26, 95% confidence interval [CI] = 1.08–1.47, $p = 0.003$), body mass index (OR = 1.97, 95% CI = 1.20–3.22, $p = 0.007$), and cystatin-c level (OR = 1.22, 95% CI = 1.07–1.39, p = 0.003) at discharge were independent risk factors for post-discharge abnormal eGFR. Plasma metabolomics at the 3-months follow-up revealed that β-pseudouridine, uridine, and 2-(dimethylamino) guanosine levels gradually increased with an abnormal degree of eGFR. Moreover, the kynurenine pathway in tryptophan metabolism, vitamin B6 metabolism, cysteine and methionine metabolism, and arginine biosynthesis were also perturbed in survivors with abnormal eGFR.

1. Introduction

The coronavirus disease (COVID-19) pandemic is rapidly unfolding worldwide and is a global public health crisis. As of March 21, 2021, it has resulted in more than 121 million confirmed cases and more than 2.6 million deaths [1]. Acute kidney injury (AKI) is a major complication of COVID-19 that occurs in 36.6%–56.9% in-hospital patients according to previous studies [2–4]. Further, AKI is a significant risk factor for mortality among patients with COVID-19 [5,6]. A recent study from the United States demonstrated that one-third of patients with COVID-19 and AKI did not recover their kidney function until a median of 21 days (interquartile range [IQR] = 8–38 days) after hospital discharge [3]. In addition, compared to patients with non-COVID-19-related AKI, those with COVID-19-related AKI had a higher rate of eGFR decline after discharge [7]. However, the glomerular filtration rate (GFR) reported in previous studies was estimated based only on the serum creatinine (Scr)

Abbreviations: eGFR, estimated glomerular filtration rate; CT, computed tomography; OR, odds ratio; CI, confidence interval; COVID-19, coronavirus disease; AKI, acute kidney injury; IQR, interquartile range; GFR, glomerular filtration rate; Scr, serum creatinine; Cys-c, cystatin c; CKD, chronic kidney disease; SARS-CoV-2, severe acute respiratory syndrome coronavirus 2; LC, liquid chromatography; MS, mass spectrometry; ESI, electrospray ionization; OPLS-DA, orthogonal partial least square-discriminant analysis; BMI, body mass index; VIP, variable importance in projection; UA, uric acid; CRP, C-reactive protein; LDH, lactate dehydrogenase; BUN, blood urea nitrogen; Kyn/Tryp, kynurenine-to-tryptophan ratio; aPL, antiphospholipid; SAH, S-adenosylhomocysteine.

* Corresponding author.
E-mail address: whuhjy@hust.edu.cn (Y. Jin).
[1] Authors contributed equally to this work.

https://doi.org/10.1016/j.bbadis.2021.166289
Received 6 May 2021; Received in revised form 4 October 2021; Accepted 8 October 2021
Available online 14 October 2021

level, and patients without AKI were not included. Thus, the long-term kidney consequences in COVID-19 survivors are largely unknown, especially in severely ill patients.

The kidney is involved in various biological functions, such as filtration, excretion, and metabolism of several bioactive substances [8]. Estimated GFR (eGFR) is the most widely used measure for the diagnosis and evaluation of kidney disease [8]. eGFR calculations based on Scr and serum cystatin C (Cys-c) levels are much more accurate than those based on either component alone [9]. A kidney biopsy study of six patients with mild COVID-19 and acute kidney injury showed that glomerular lesions mainly manifested as podocytopathy, collapsing glomerulopathy, or both [10]. Moreover, microthrombi have been observed in the peritubular capillaries and glomeruli of kidney tissues [11]. These glomerular injuries may lead to a long-term progressive decline in the GFR, ultimately leading to the occurrence of end-stage renal disease. Thus, early detection and accurate monitoring of eGFR decline in patients with COVID-19 could improve care and delay progression to end-stage renal disease.

Recently, metabolomics has been widely used to identify of the molecular diagnostic markers and unravel the pathological mechanisms of chronic kidney disease (CKD) [12]. Differential metabolites indicate distinct etiologies of CKD, such as proteinuria, diet, and drug use, and may lead to elucidation of novel disease-specific therapeutic targets or potential early, non-invasive diagnostic techniques [13]. Huang et al. recently reported that among the 822 COVID-19 survivors without AKI who had an eGFR $\geq$90 mL/min per 1.73 m^2 in the acute phase of COVID-19, 107 (13.02%) had an eGFR<90 mL/min per 1.73 m^2 within 6 months of disease onset [14]. In addition, we have previously revealed the plasma metabolomic characteristics of patients with COVID-19 and pulmonary sequelae at 3 months after discharge [15]. Therefore, based on this research, we sought to further explore the changes in eGFR (calculated based on Scr and serum Cys-c levels) in severely ill COVID-19 survivors from hospitalization to 3 months after hospital discharge and their metabolomic differences associated with renal function. None of the patients had received continuous renal replacement therapy before the study period, but all patients had received nasal catheter oxygen inhalation during hospitalization, including those who received mechanical ventilation.

2. Methods

2.1. Study participants

This study included 89 patients with severe COVID-19 who were discharged from the Wuhan Union Hospital sequentially in mid-to-late March 2020. They had no underlying kidney disease before admission. All patients were recruited in mid-to-late June 2020, approximately 3 months after discharge and 4.5–5 months after disease onset. All patients were diagnosed and classified as having severe disease according to the World Health Organization interim guidelines when they were hospitalized [16].

Data on the following demographic and clinical characteristics were collected: age, sex, body mass index (BMI), comorbidities, therapy history, laboratory findings, and lung computed tomography (CT) findings during hospitalization. Routine blood tests, severe acute respiratory syndrome coronavirus 2 (SARS-CoV-2) antibody detection test, blood biochemical tests (renal and liver function markers), and coagulation tests were performed at 3 months after discharge. We also collected peripheral blood samples and stored them at −80 °C for subsequent metabolite detection.

The study was performed in accordance with the Declaration of Helsinki and was registered on the Clinical Trials website (No. NCT04456101). The study protocol was reviewed and approved by the Institutional Review Boards of the Medical Ethics Committee of Wuhan Union Hospital (NO. 0271-01). All participants or their surrogates provided informed consent.

2.2. eGFR calculation and patient grouping

To assess the results of renal function more accurately, we calculated the eGFR based on Scr and Scys-c levels using the CKD-EPI formula [9]. An eGFR of <90 mL/min per 1.73 m^2 was considered abnormal. Patients were subsequently divided into three groups according to the different eGFR change patterns—NNeGFR (normal eGFR both during hospitalization and 3 months after discharge, $n = 20$), NAeGFR (normal eGFR during hospitalization but abnormal at 3 months after discharge, $n = 25$), and AAeGFR (abnormal eGFR during hospitalization and 3 months after discharge, $n = 44$).

2.3. Sample collection and metabolomic profiling

All participants were instructed to fast for 12 h prior to blood sampling and not to take any medications or dietary supplements within 48 h before blood sampling. Peripheral venous blood was collected in ethylenediaminetetraacetic acid-coated vacutainer tubes and centrifuged at 2000 rpm for 10 min at 4 °C to obtain plasma samples, which were immediately stored at −80 °C and used for metabolomic profiling later.

The liquid chromatography (LC)–electrospray ionization (ESI)–mass spectrometry (MS)/MS system (Shim-pack UFLC SHIMADZU CBM A UPLC system, coupled with QTRAP® 6500+ System MS) was used to measure metabolites in the fasting plasma samples. To detect as many metabolites as possible, both hydrophilic and hydrophobic metabolites were extracted and analyzed. Briefly, plasma samples were thawed on ice, and the hydrophilic and hydrophobic metabolites were extracted with ice methanol and lipid extract, respectively. A quality control sample was prepared in advance, and analyzed after every 10 study samples in the LC-MS/MS running sequence to evaluate the stability of LC-MS/MS analysis. MS analysis of hydrophilic and hydrophobic metabolites was performed in the positive and negative ion modes and controlled using Analyst software (SCIEX Analyst, version 1.6.3). Detailed information about metabolite detection process using the LC-ESI-MS/MS system was the same as that reported in previous studies [15,17]. Metabolite identification and quantification were performed using a self-made database with retention times and ion pairs. For metabolites without authentic standards in our database, we used MS/MS spectra to search public databases to increase confidence in metabolite identification. Orthogonal partial least square-discriminant analysis (OPLS-DA) was used to distinguish the metabolomic profiles between patient groups with different eGFR change patterns.

2.4. Screening of differential metabolites and analysis of metabolic pathways

OPLS-DA was performed using SIMCA-P software (version 11.0; Umetrics). For comparison of metabolite profiles between any two groups, Mann–Whitney *U* test was performed to obtain *p* values and infer significance. Variable importance in projection (VIP) scores were also calculated. Differential metabolites were screened using $p < 0.05$, VIP > 1, and fold change (FC) > 1.2 or FC < 0.83.

To map the metabolic pathways of metabolites ($p < 0.05$, VIP > 1, and FC > 1.2 or FC < 0.83) with significant changes between the AAeGFR and NNeGFR groups and between the AAeGFR and NAeGFR groups, enrichment analysis and visualization of metabolic pathways was performed using the online software Metaboanalyst (https://www.metaboanalyst.ca/MetaboAnalyst/).

2.5. Statistics

Associations between the differential metabolites and clinical indices were examined using Spearman correlation analysis and visualized on corresponding correlation matrix plots or scatter plots. Heatmaps of differential metabolites between any two groups were displayed using

Multi Experiment Viewer software (MeV, version 4.7.4).

Clinical data are reported as medians and IQRs for continuous variables and as counts and percentages for categorical variables. To compare the differences in clinical variables among the three groups at each time point, we used the Kruskal–Wallis test for continuous variables and the chi-square test or Fisher's exact test for categorical variables. The paired Wilcoxon signed–rank test was used to compare the differences in each variable at discharge and 3 months after discharge. Univariable and multivariable logistic regression analyses were used to compare patients with or without abnormal eGFR at 3 months after discharge. All tests were two sided, and a p value of <0.05 was considered statistically significant All statistical analyses were performed using SPSS version 26.

Table 1
Clinical characteristics of severely ill COVID-19 survivors with different eGFR change patterns from hospitalization to 3 months after discharge.

Characteristics	Total (n = 89)	Normal eGFR	Abnormal eGFR (n = 69) [77.5%]		p value
		NNeGFR (n = 20) [22.5%]	NAeGFR (n = 25) [28.1%]	AAeGFR (n = 44) [49.4%]	
Age, median (*IQR*), years	61.5 (55.0–69.0)	52.0 (43.3–57.0)	56.0 (54.0–63.0)	68.0 (61.0–68.0)	<0.0001
Sex (male), n (%)	40 (44.9%)	6 (30.0%)	9 (36.0%)	25 (56.8%)	0.077
BMI, median (*IQR*), kg/m^2	24.2 (22.3–26.1)	22.4 (21.2–24.2)	24.2 (22.8–26.4)	25.0 (23.0–26.6)	0.014
Comorbidities					
Chronic respiratory disease	0	0	0	0	–
Chronic kidney disease	0	0	0	0	–
Hypertension	30 (33.7%)	3 (15.0%)	3 (12.0%)	24 (54.5%)	<0.0001
Diabetes	19 (21.3%)	4 (20.0%)	4 (16.0%)	11 (25.0%)	0.671
Coronary heart disease	9 (10.1%)	2 (10%)	0 (0%)	7 (15.9%)	0.091[a]
Cerebrovascular disease	4 (4.5%)	1 (5.0%)	1 (4.0%)	2 (4.5%)	1.00[a]
Malignancy	3 (3.4%)	0 (0%)	2 (8.0%)	1 (2.3%)	0.315[a]
Liver disease	8 (9.0%)	1 (5.0%)	1 (4.0%)	6 (13.6%)	0.436[a]
Days from disease onset to admission	11.0 (9.0–15.0)	11.0 (8.5–15.0)	11.0 (8.5–14.0)	12.0 (9.0–15.0)	0.849
Days of hospital stay	39.0 (32.0–47.0)	35.5 (23.8–43.0)	39.0 (23.5–48.5)	40.0 (35.5–47.3)	0.158
Antiviral therapy	45/87 (51.7%)	14 (70.0%)	13 (52.0%)	18/42 (42.9%)	0.135
Arbidol	42/87 (48.3%)	12 (60.0%)	12 (48.0%)	18/42 (42.9%)	0.450
Oseltamivir	3/87 (3.4%)	1 (5.0%)	0 (0%)	2/42 (4.8%)	0.599[a]
Interferon	11/87 (12.6%)	2 (10.0%)	4 (16.0%)	5/42 (11.9%)	0.838[a]
Lopinavir and ritonavir tablets	13/87 (14.9%)	2 (10.0%)	4 (16.0%)	7/42 (16.7%)	0.857[a]
Ribavirin	11/87 (12.6%)	3 (15.0%)	4 (16.0%)	4/42 (9.5%)	0.701[a]
Antibacterial therapy	40/87 (46.0%)	12 (60.0%)	11 (44.0%)	17/42 (40.5%)	0.344
Corticosteroids	22/87 (25.3%)	5 (25.0%)	5 (20.0%)	12/42 (28.6%)	0.737
Intravenous immunoglobulin	9/87 (10.3%)	2 (10.0%)	4 (16.0%)	3/42 (7.1%)	0.484[a]
Continuous renal replacement therapy	0	0	0	0	–
Oxygen therapy					
Nasal catheter/face mask	89 (100%)	20 (100%)	25 (100%)	44 (100%)	–
High-flow oxygen therapy	32 (36.0%)	5 (25.0%)	8 (32.0%)	19 (43.2%)	0.33
Non-invasive ventilation	6 (6.7%)	2 (10.0%)	2 (8.0%)	2 (4.5%)	0.638[a]
Intubation	4 (4.5%)	0 (0%)	0 (0%)	4 (9.1%)	0.179[a]
Antibodies of SARS-CoV2 at 3 months after discharge					
IgM positive	13/86 (15.1%)	3 (15.0%)	3/24 (12.5%)	7/42 (16.7%)	0.927[a]
IgG positive	84/86 (97.7%)	19 (95.0%)	24/24 (100%)	41/42 (97.6%)	0.489[a]
eGFR (CKD-EPIscr-cys, mL/min per 1.73 m^2), [normal range: ≥90]					
At admission	95.4 (78.5–108.1)	117.3 (110.4–121.2)	105.8 (97.9–109.3)	79.4 (71.4–85.8)	<0.0001
Mid-hospitalization	95.0 (76.8–105.1)	116.8 (111.4–118.6)	102.0 (98.3–107.1)	77.5 (72.1–87.5)	<0.0001
At discharge	93.2 (81.8–104.0)	115.1 (105.1–120.6)	102.9 (99.0–106.3)	82.0 (72.3–88.7)	<0.0001
3 months after discharge	76.8 (66.0–87.7)	96.9 (94.3–108.6)	82.6 (79.0–87.1)	67.2 (55.6–74.9)	<0.0001
Cystatin C (mg/L), [normal range: 0.55–1.05 mg/L]					
At admission	0.80 (0.73–0.99)	0.65 (0.60–0.77)	0.78 (0.70–0.79)	0.97 (0.82–1.12)	<0.0001
Mid-hospitalization	0.87 (0.77–1.01)	0.69 (0.63–0.80)	0.80 (0.75–0.86)	1.0 (0.91–1.14)	<0.0001
At discharge	0.86 (0.78–1.02)	0.68 (0.60–0.80)	0.81 (0.75–0.85)	0.98 (0.91–1.11)	<0.0001
3 months after discharge	1.09 (0.94–1.30)	0.83 (0.76–0.88)	1.04 (0.94–1.10)	1.21 (1.12–1.40)	<0.0001
Serum creatinine (μmol/L), [normal range: 41–81 μmol/L]					
At admission	68.0 (56.1–78.1)	53.1 (43.0–59.7)	58.2 (53.2–70.4)	74.7 (67.7–87.8)	<0.0001
Mid-hospitalization	62.6 (52.9–74.3)	49.4 (43.8–55.5)	57.7 (52.1–63.5)	73.0 (61.8–85.9)	<0.0001
At discharge	62.2 (54.5–78.0)	53.5 (43.2–59.5)	55.9 (50.8–66.2)	69.7 (60.2–83.1)	<0.0001
3 months after discharge	70.5 (63.7–80.3)	62.3 (56.8–67.5)	65.2 (62.5–74.2)	75.0 (69.3–98.5)	<0.0001

Note: Data were presented as median (*IQR*) for continuous variables and n (%) for category variables. Kruskal–Wallis (K-W) test was used for analysis of continuous variables and chi-square test or fisher's exact test for analysis of all category variables between three groups.

Abbreviations: eGFR: estimated glomerular filtration rate; normal eGFR denotes that eGFR was normal (≥90 mL/min per 1.73 m^2) at three months after discharge. Abnormal eGFR denotes that eGFR was abnormal (<90 mL/min per 1.73 m^2) at three months after discharge.

Three change patterns of eGFR from hospitalization to 3 months after discharge, they are NNeGFR: normal estimated glomerular filtration rate (eGFR) during hospitalization and at 3 months after discharge; NAeGFR: normal eGFR during hospitalization, but abnormal eGFR at 3 months after discharge; AAeGFR: abnormal eGFR during hospitalization and at 3 months after discharge; IQR: interquartile range; BMI: body mass index.

[a] Fisher's exact test.

3. Results

3.1. eGFR change patterns and other clinical variables among severely ill COVID-19 survivors 3 months after discharge

In this study, 89 patients who recovered from severe COVID-19 were classified into three groups according to their kidney function. There were 20, 25, and 44 patients in the NNeGFR, NAeGFR, and AAeGFR groups, respectively. None of the patients had received continuous renal replacement therapy before the study period, but all patients had received nasal catheter oxygen inhalation during hospitalization. Among them, 10 (11.2%) patients received mechanical ventilation, including four (4.5%) patients who received intubation and six (6.7%) patients who received non-invasive mechanical ventilation (Table 1).

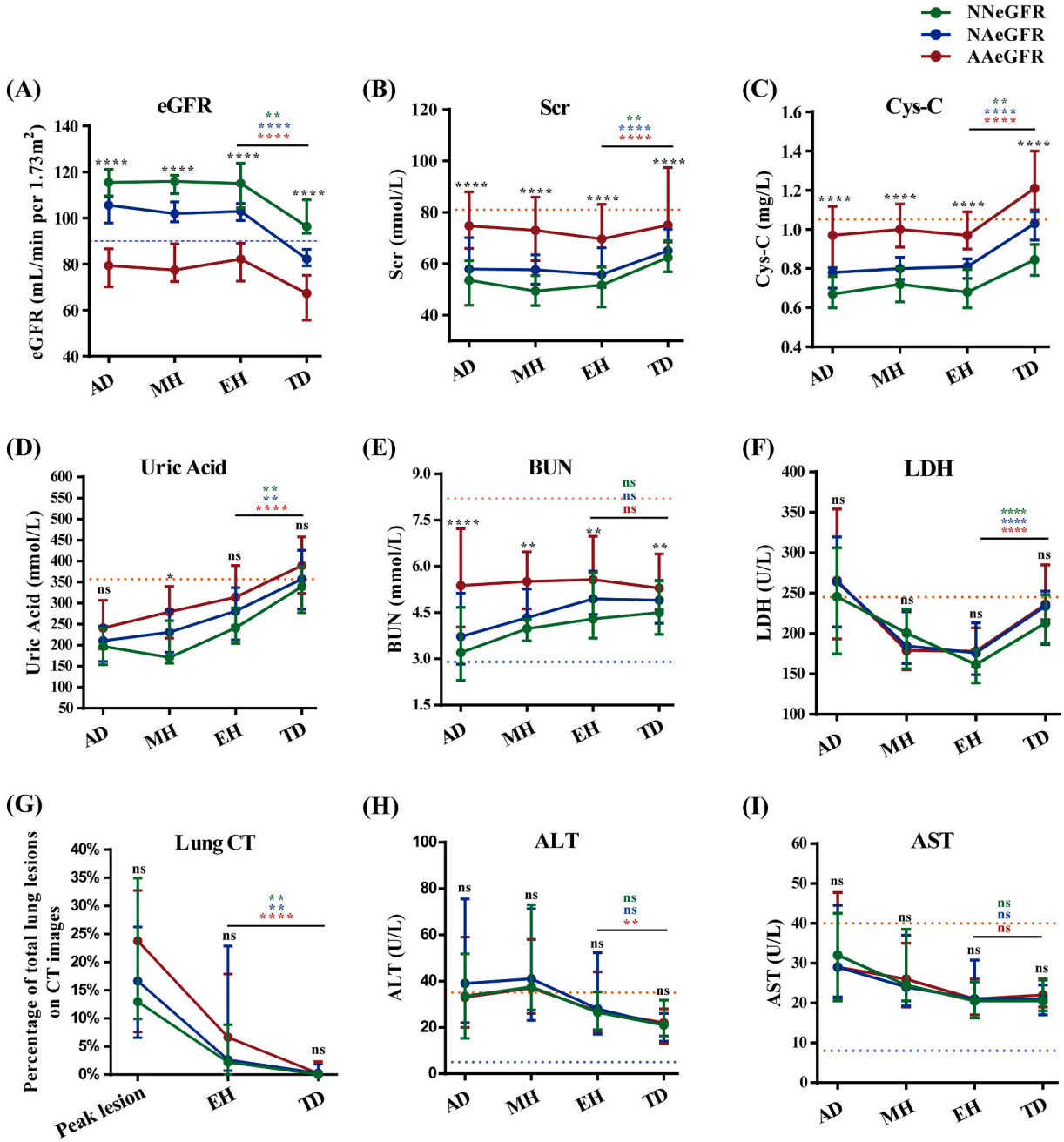

Fig. 1. Dynamic changes in representative clinical indicators in severely ill COVID-19 survivors with different eGFR change patterns (NNeGFR, NAeGFR, and AAeGFR).

Clinical indicators are analyzed at four time points: at admission (AD), mid-hospitalization (MH), end of hospitalization (EH) and 3 months after discharge (TD). The median value with the interquartile range of clinical indicators at each time point is displayed. Significant differences among the groups at each time point are compared using the Kruskal–Wallis test, and the significant change between the EH and TD is compared using the Wilcoxon signed rank test for correlated samples. The *p* value is indicated as ns, no significance; *, <0.05; **, <0.01; ***, <0.001; and ****, <0.0001. The horizontal red dotted line and the horizontal blue dotted line represent the upper and lower limits of the reference range for each indicator, respectively.

NNeGFR: normal estimated glomerular filtration rate (eGFR) during hospitalization and at 3 months after discharge; NAeGFR: normal eGFR during hospitalization, but abnormal eGFR at 3 months after discharge; AAeGFR: abnormal eGFR during hospitalization and at 3 months after discharge; Scr, serum creatinine; Cys-c, Cystatin C; BUN, blood urea nitrogen; LDH, lactate dehydrogenase; ALT, alanine transaminase; AST, aspartate transaminase. (For interpretation of the references to color in this figure legend, the reader is referred to the web version of this article.)

The median time from disease onset to admission and of hospitalization was 11.0 (IQR = 9.0–15.0) days and 39.0 (IQR = 32.0–47.0) days, respectively (Table 1). The characteristics of the three groups are summarized in Table 1. The mean age of the study population was 61.5 (IQR = 55.0–69.0) years, and patients in the AAeGFR group were significantly older than those in the other two groups. The NNeGFR group had a lower BMI than the NAeGFR and AAeGFR groups. The prevalence of hypertension was significantly higher in the AAeGFR group than in the NNeGFR or NAeGFR groups. Therapy history, including antiviral, antibacterial, corticosteroids, and intravenous immunoglobulin therapy, showed no significant difference among patients with different eGFR change patterns.

However, the eGFR, cystatin-c (Cys-c), and Scr level at four time points (at admission, AD; mid-hospitalization, MH; end-hospitalization, EH; and 3 months after discharge, TD) were significantly different among the three groups of patients (all $p < 0.0001$) (Table 1). At 3 months after discharge, the eGFR decreased significantly in all groups. The levels of other renal function markers, such as Scr, Cys-c, and uric acid (UA), were significantly increased, while chest CT findings, liver function, inflammatory factors, and coagulation indicators showed a trend toward recovery at 3 months after discharge (Fig. 1). Moreover, renal markers in all groups showed a trend of parallel changes from hospitalization to 3 months after discharge. The renal function in the AAeGFR group was the worst throughout, but other organ indicators showed no obvious discrepancies among the three groups at the four time points (Fig. 1 and Fig. S1).

3.2. Clinical features and risk factors of severely ill COVID-19 survivors with abnormal eGFR 3 months after discharge

Clinical features were compared between severely ill COVID-19 survivors with normal eGFR (NNeGFR group) and abnormal eGFR (NAeGFR group and AAeGFR group) at 3 months after discharge (Table 2). The univariable analysis indicated that age (odds ratio [OR] = 1.15, $p < 0.0001$), BMI (OR = 1.34, $p = 0.011$), platelet counts (OR = 0.99, $p = 0.031$), eGFR (OR = 0.84, $p < 0.0001$), Cys-c level (OR = 1.17, $p < 0.0001$), Scr level (OR = 1.11, $p = 0.001$), blood urea nitrogen (BUN) level (OR = 2.20, $p = 0.004$), lactate dehydrogenase (LDH) level (OR = 1.02, $p = 0.032$), and C-reactive protein (CRP) level (OR = 1.51, $p = 0.017$) at discharge were significantly different between patients with normal and abnormal eGFR at 3 months after discharge. Multivariable analysis showed that age (OR = 1.26, 95% confidence interval [CI] = 1.08–1.47, $p = 0.003$), BMI (OR = 1.97, 95% CI = 1.20–3.22, $p = 0.007$), and Cys-c level (OR = 1.22, 95% CI = 1.07–1.39, $p = 0.003$) at discharge were independent risk factors associated with abnormal eGFR at 3 months after discharge.

3.3. Metabolomic differences between severely ill COVID-19 survivors with different eGFR change patterns 3 months after discharge

Metabolomic profiling using plasma samples was completed in 69 patients (15 in the NNeGFR group, 18 in the NAeGFR group, and 36 in the AAeGFR group). We identified 554 hydrophilic and 590 hydrophobic metabolites in the plasma samples, among which 35 were both

Table 2
Risk factors at discharge associated with abnormal eGFR at 3 months after discharge among patients recovered from severe COVID-19.

Variables at discharge	eGFR at 3 months after discharge		Univariable analysis	P value	Multivariable analysis	P value
	Normal (n = 20) ≥90 ml/min*173 m^2	Abnormal (n = 69) <90 ml/min*173 m^2	OR (95% CI)		OR (95% CI)	
Age, years	52.00 (43.25–57.00)	64.00 (56.50–70.00)	1.15 (1.07–1.23)	<0.0001	1.26 (1.08–1.47)	0.003
Sex (male)	6 (30.0%)	34 (49.3%)	2.27 (0.78–6.59)	0.133		
BMI	22.36 (21.16–24.19)	24.77 (23.03–26.56)	1.34 (1.07–1.67)	0.011	1.97 (1.20–3.22)	0.007
Hypertension	3 (15.0%)	27 (39.1%)	3.64 (0.97–13.63)	0.055		
Diabetes	4 (20.0%)	15 (21.7%)	1.11 (0.32–3.82)	0.87		
Lesion% on lung CT	2.22 (0.05–8.87) %	4.81 (1.34–17.74) %	1.08 (0.99–1.17)	0.086		
Hemoglobin, g/L	120.50 (109.50–129.50)	123.50 (113.25–134.75)	1.02 (0.98–1.05)	0.387		
Platelets, ×109/L	260.50 (192.75–287.75)	208.50 (173.25–248.75)	0.99 (0.98–1.00)	0.031		
Neutrophils, ×109/L	3.38 (2.59–4.15)	3.29 (2.68–4.50)	1.04 (0.70–1.54)	0.84		
Lymphocytes, ×109/L	1.75 (1.47–1.92)	1.60 (1.26–2.06)	0.95 (0.43–2.09)	0.95		
NLR	2.15 (1.48–2.87)	2.00 (1.61–2.66)	1.14 (0.78–1.67)	0.504		
TBIL, μmol/L	8.95 (7.25–12.25)	10.20 (7.80–12.90)	1.03 (0.90–1.19)	0.665		
ALT, U/L	26.50 (19.00–35.25)	27.00 (17.00–45.00)	1.00 (0.99–1.03)	0.488		
AST, U/L	20.50 (16.25–25.25)	21.00 (17.00–27.00)	1.03 (0.97–1.10)	0.298		
ALP, U/L	56.50 (53.00–70.75)	61.00 (52.00–74.00)	1.01 (0.97–1.04)	0.660		
γ-GT, U/L	28.50 (17.75–34.50)	30.00 (20.00–47.00)	1.02 (0.99–1.06)	0.155		
Total protein, g/L	67.40 (64.60–70.05)	66.60 (64.10–70.80)	0.96 (0.87–1.06)	0.396		
Albumin, g/L	38.65 (36.00–42.48)	39.80 (36.70–41.80)	1.00 (0.89–1.14)	0.945		
Albumin/globin	1.35 (1.18–1.70)	1.50 (1.30–1.70)	1.58 (0.30–8.45)	0.591		
eGFR, mL/min per 1.73 m^2	115.12 (104.48–123.91)	89.54 (79.23–100.67)	0.84 (0.76–0.92)	<0.0001		
Cystatin C, μg/dL	68 (60–80)	90 (81–103)	1.17 (1.08–1.26)	<0.0001	1.22 (1.07–1.39)	0.003
mg/L	0.68 (0.60–0.80)	0.90 (0.81–1.03)				
Serum creatinine, μmol/L	51.70 (43.18–58.68)	63.90 (56.00–79.60)	1.11 (1.04–1.17)	0.001		
BUN, mmol/L	4.30 (3.67–5.79)	5.40 (4.62–6.46)	2.20 (1.28–3.79)	0.004		
UA, μmol/L	241.15 (204.43–289.13)	289.00 (229.10–382.20)	1.01 (1.00–1.01)	0.083		
LDH, U/L	161.50 (138.75–180.00)	178.00 (155.00–208.00)	1.02 (1.00–1.04)	0.032		
CRP, mg/L	0.10 (0.10–2.26)	3.40 (0.10–4.86)	1.51 (1.08–2.11)	0.017		
D-dimer, μg/ml	0.27 (0.19–0.59)	0.34 (0.23–0.78)	0.95 (0.52–1.76)	0.877		
PT, seconds	12.80 (12.38–13.75)	12.40 (12.10–13.35)	0.99 (0.78–1.26)	0.937		
APTT, seconds	37.10 (35.03–41.75)	36.00 (33.88–39.63)	1.01 (0.93–1.09)	0.912		
FIB, g/l	2.92 (2.51–3.51)	3.46 (2.98–3.88)	2.66 (0.95–7.40)	0.062		
TT, seconds	15.75 (15.13–16.08)	15.40 (14.68–16.40)	0.90 (0.50–1.65)	0.738		

Note: Data were presented as median (IQR) for continuous variables and n (%) for category variables. Univariable and multivariable logistic regression analysis were employed for the comparison of variables at discharge between patients with normal or abnormal eGFR three months after discharge.
Abbreviations: BMI: body mass index, NLR: neutrophil-to-lymphocyte ratio, TBIL: total bilirubin, ALT: alanine aminotransferase, AST: aspartate aminotransferase, ALP: alkaline phosphatase, γ-GT: γ-glutamyl transpeptidase, eGFR: Estimated Glomerular Filtration Rate, BUN: blood urea nitrogen, UA: urine acid, LDH: lactate dehydrogenase, CRP: C-reactive protein, PT: prothrombin time, APTT: activated partial thromboplastin time, FIB: fibrinogen, TT: thrombin time.

perturbed ($P < 0.05$, FC > 1.2 or FC < 0.83, and VIP > 1) in the AAeGFR vs. NNeGFR and AAeGFR vs. NAeGFR groups (Table S1, Fig. 2A–C). In the OPLS-DA plot, plasma samples from AAeGFR group patients were separated from those from NNeGFR and NAeGFR group patients, indicating that the metabolic profiles of AAeGFR group patients were remarkably different from those of the NNeGFR and NAeGFR group patients (Fig. 2A). Compared to the NNeGFR and NAeGFR groups, the AAeGFR group had decreased levels of PC(O-18:2/18:1), PC(O-20:4/20:4), PS(18:2/20:0), PE(P-18:1/16:0), and PE(P-18:2/18:1) and increased levels of other 30 metabolites including amino acids,

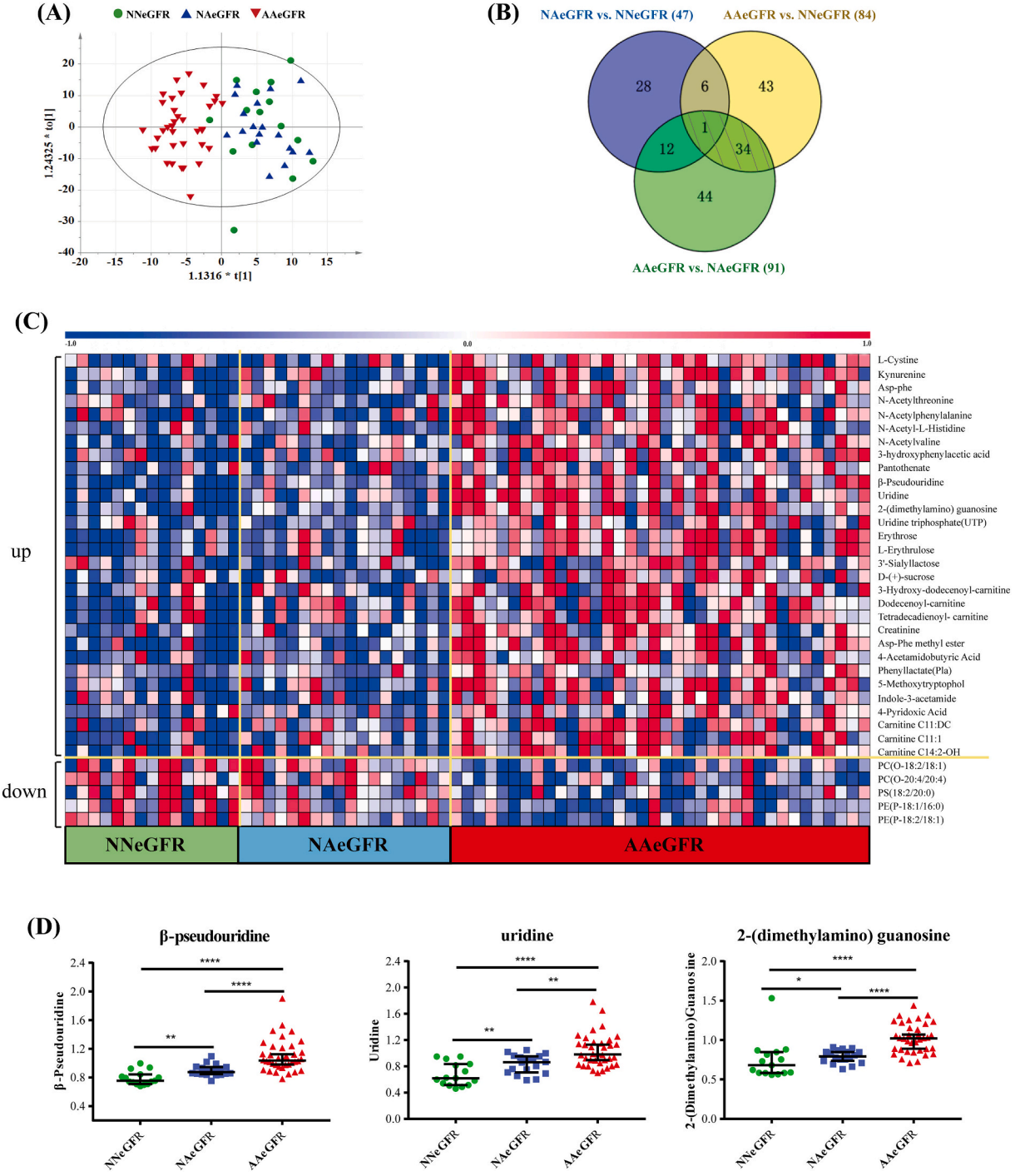

Fig. 2. Metabolites profiling of plasma samples from patients with severe COVID-19 discharged from hospital before 3 months with different eGFR change patterns (NNeGFR, NAeGFR and AAeGFR).

(A) Score plots of orthogonal partial least square-discriminant analysis (OPLS-DA) based on 553 hydrophilic and 590 hydrophobic metabolites detected in the three groups. (B) Venn diagram showing the number of differential metabolites in NNeGFR, NAeGFR and AAeGFR group patients. (C) Heat map of 35 differential metabolites in NAeGFR and AAeGFR group patients compared to those in NNeGFR group patients. Only differential metabolites with $P < 0.05$, FC > 1.2 or FC < 0.83, and VIP > 1 are displayed, and the shades of the color indicate the level of metabolites (white denotes the mean level and blue and red denote a relatively lower and higher level, respectively). (D) Change in the expression levels of three typical metabolites among the groups. Asterisks indicate statistical significance based on the Mann–Whitney *U* test. The *p* value is indicated as ns, no significance; *, <0.05; **, <0.01; ***, <0.001; and ****, <0.0001. (For interpretation of the references to color in this figure legend, the reader is referred to the web version of this article.)

nucleotides, carboxylic acids, and lipids (Fig. 2C). β-Pseudouridine, uridine and 2-(dimethylamino) guanosine were the metabolites gradually increased in the plasma of the three group patients (Fig. 2D). All these evidences revealed the pathological metabolic markers underlying the renal sequelae of COVID-19.

3.4. Differences in metabolic pathways among patients with abnormal eGFR 3 months after discharge

To further analyze the metabolomic data, we performed KEGG pathway enrichment analysis to annotate the potential functional implication of differential metabolites between the AAeGFR vs. NNeGFR and AAeGFR vs. NAeGFR groups (Fig. 3A, B). The differential metabolites of the AAeGFR vs. NNeGFR group were enriched in 19 metabolic pathways, while those of the AAeGFR vs. NAeGFR group were enriched in 21 metabolic pathways. Four relatively top-ranked pathways reported to be highly correlated with renal function were highlighted, including the cysteine and methionine metabolism, vitamin B6 metabolism, tryptophan metabolism, and arginine biosynthesis pathways. Among them, vitamin B6 metabolism and tryptophan metabolism pathways were both enriched in the AAeGFR vs. NNeGFR and AAeGFR vs. NAeGFR groups. The details of the four metabolic pathways closely related to renal function are shown in Fig. 3C–F. The kynurenine-to-tryptophan ratio (Kyn/Tryp), which plays an important role in tryptophan metabolism, and the level of 4-pyridoxic acid, the main terminal metabolite of B6 metabolism, were significantly higher in the AAeGFR group than in the NNeGFR and NAeGFR groups (Fig. 3C, D). In addition, the levels of L-cystine, the main metabolite of cysteine and methionine metabolism, and urea, a metabolite in the urea cycle, were higher in the AAeGFR and NAeGFR groups than in the NNeGFR group (Fig. 3E, F).

3.5. Correlation between renal function markers and differential metabolites

To further understand the relationship between the metabolites altered in the AAeGFR vs. NNeGFR and AAeGFR vs. NAeGFR groups and the phenotype of renal function, correlation analysis of these differential metabolites with relevant clinical indices, including eGFR, cystatin C, creatinine, BUN, UA, CRP, and LDH, was performed (Fig. 4A–D). We observed that β-pseudouridine, 2-(dimethylamino) guanosine, Asp-Phe, uridine, 4-acetamidobutyric acid, Asp-Phe methyl ester, creatinine (mass spectrometry), kynurenine, 5-methoxytryptophol (5-MTP), *N*-acetylphenylalanine, and *N*-acetylthreonine displayed significant negative correlations with eGFR and positive correlations with cystatin C and creatinine (clinical) (all $|r| > 0.5$, and $p < 0.05$) (Fig. 4B–D). This suggested that the elevation of these metabolites in plasma was associated with aggravated renal functions.

4. Discussion

Our results demonstrated that the eGFR (calculated based on Scr and Cys-c levels) significantly decreased at 3 months after discharge in severely ill COVID-19 survivors, especially in patients whose eGFR was abnormal during hospitalization, but their chest CT findings, liver function, inflammatory factors, and coagulation indicators showed a trend toward recovery at 3 months after discharge. Pathway analysis revealed that alterations related to eGFR mainly involved the tryptophan metabolism, vitamin B6 metabolism, cysteine and methionine metabolism, arginine biosynthesis (urea cycle), and glycerophospholipid metabolism pathways. This suggests that metabolic alterations are a marker of more abnormal eGFR in COVID-19 survivors.

eGFR based on Scr and serum Cys-c levels, which was used to indicate renal sequelae of severe COVID-19 in this study, has been proven to be a confirmatory test for CKD [9]. Our study revealed that age, BMI, and Cys-c levels at discharge were independent risk factors associated with abnormal eGFR at 3 months after discharge among severely ill COVID-19 survivors. Furthermore, metabolomic alterations were significant among AAeGFR group patients compared to those in NNeGFR and NAeGFR group patients. In particular, alterations in metabolites involved in tryptophan metabolism, cysteine and methionine metabolism, and vitamin B6 metabolism, such as kynurenine, indole-3-acetamid, 5-MTP, and 4-pyridoxic acid, were remarkably related to changes in renal function. In addition, the levels of three typical metabolites—β-pseudouridine, uridine, and 2-(dimethylamino) guanosine—increased gradually in the three groups. Altered production or urinary excretion can change the plasma concentrations of small organic metabolites [18]. Thus, the alterations in these metabolites might have been caused by the reduced eGFR in patients with severe COVID-19.

In a previous study, antiphospholipid (aPL) autoantibodies were present in 52% serum samples from 172 hospitalized patients with COVID-19, and higher titers of aPL antibodies were associated with lower clinical eGFR [19]. In other previous studies, many patients with COVID-19 and AKI did not fully recover their renal function [3,6]. Evidence suggest that SARS-CoV-2 particles can invade podocytes manifesting as foot process effacement, occasional vacuolation, and detachment of podocytes from the glomerular basement membrane in kidney tissues of autopsy specimens [20]. Moreover, studies have shown that microthrombi are found in the kidney cortex of autopsy specimens from patients with COVID-19 [11]. Additionally, it has been proven that acute injury would cause damage to peritubular capillaries in the kidney, which can permanently alter renal function and increase susceptibility to chronic renal insufficiency [21,22].

Pseudouridine is the C-glycosidic derivative of uridine, a modified nucleoside found in RNA [23]. Increased pseudouridine levels have been associated with kidney function decline and incident CKD, and pseudouridine has been shown to be a better biomarker than creatinine for CKD stratification [24]. Uridine metabolism is closely related to glucose homeostasis and lipid and amino acid metabolism [25]. In a previous study, patients with uremia had marked accumulation of uridine due to altered RNA metabolism [26]. In our study, the plasma levels of β-pseudouridine and uridine increased sequentially in the NNeGFR, NAeGFR, and AAeGFR groups. This suggested the degree of impairment of renal function in severely ill COVID-19 survivors at 3 months after discharge. In addition, plasma 4-pyridoxic acid, a main metabolites of vitamin B6, is significantly elevated in patients with renal insufficiency, and the renal clearance of 4-pyridoxic acid is approximately two times higher than that of creatinine [27]. In our study, plasma 4-pyridoxic acid levels were significantly higher in the AAeGFR group than in the NNeGFR and NAeGFR groups, indicating that the increase in plasma 4-pyridoxic acid was consistent with the abnormality of eGFR.

The association between CKD in diabetic patients and accumulation of toxic tryptophan metabolites and relationship between increased kynurenine levels and CKD progression have been suggested [28,29]. Kynurenine is an endothelium-derived vasodilation factor produced during inflammation [30]. It plays an important role in the regulation of vascular function in inflammatory conditions by relaxing arterial vessels and controlling blood pressure [31,32]. Kynurenine, through its role in the regulation of vascular function, may contribute to CKD progression. Moreover, elevated plasma levels of kynurenine are considered a global diagnostic biomarker for CKD, regardless of the patient's geographic origin [33]. Further, Thomas et al. reported that the kynurenine pathway in tryptophan metabolism was the primary pathway affected by COVID-19. Kynurenine pathway abnormality is associated with renal insufficiency and disease severity, especially in patients with high interleukin-6 levels, indicating that abnormality in tryptophan metabolism is closely related to the inflammation and immune status of patients during the acute phase of COVID-19 [34]. Similarly, a recent study reported that the kynurenine pathway was significantly activated in patients infected with SARS-CoV-2, which regulates immune responses in a vigorous manner [35]. Therefore, the altered tryptophan metabolism that persists in patients recovered from COVID-19 with abnormal eGFR suggests a relatively active and abnormal inflammatory response

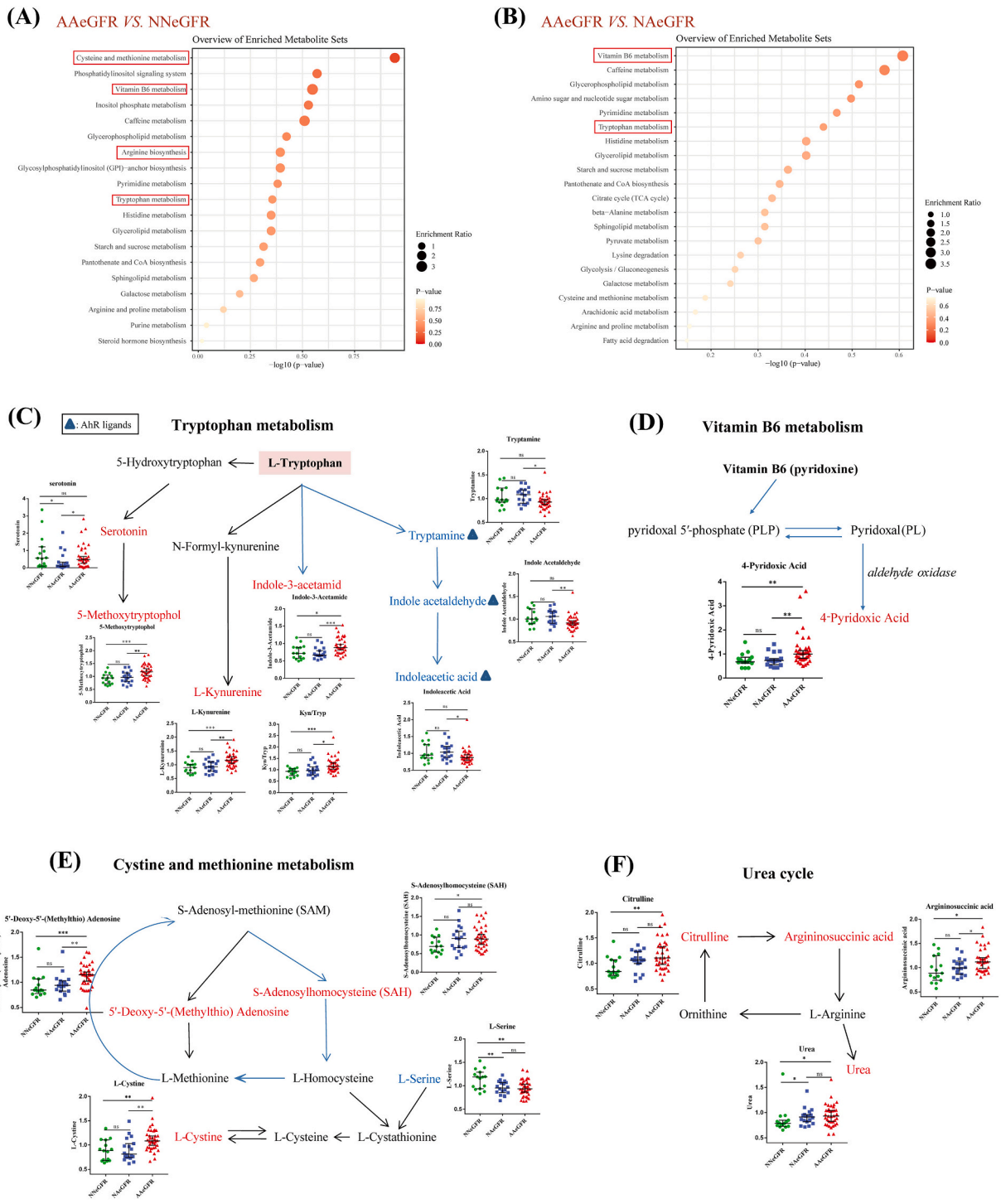

Fig. 3. Metabolic pathway analysis of patients with severe COVID-19 discharged from hospital before 3 months with different eGFR change patterns (NNeGFR, NAeGFR and AAeGFR).

(A, B) KEGG pathway enrichment analysis of differential metabolites between the AAeGFR and NNeGFR groups (A) and between the AAeGFR and NAeGFR groups (B). The color of bubbles represents the *p* value, and the size of bubbles represents the enrichment ratio of metabolites. KEGG pathways are ranked according to the *p* value and enrichment ratio. The red box indicates the relatively top-ranked pathways enriched in the AAeGFR vs. NNeGFR and AAeGFR vs. NAeGFR groups or both. (C–F) The main disordered pathways selected based on the above KEGG pathway analysis, they are Tryptophan metabolism (C), vitamin B6 metabolism (D), cysteine and methionine metabolism (E), and Urea cycle (arginine biosynthesis) (F) pathways. All significantly changed metabolites are marked in red or blue, and the corresponding scatter plots are also displayed. The Mann–Whitney U test is used for the comparison of any two groups. Asterisks indicate statistical significance based on the Mann–Whitney U test. The *p* value is indicated as ns, no significance; *, <0.05; **, <0.01; ***, <0.001; and ****, <0.0001. (For interpretation of the references to color in this figure legend, the reader is referred to the web version of this article.)

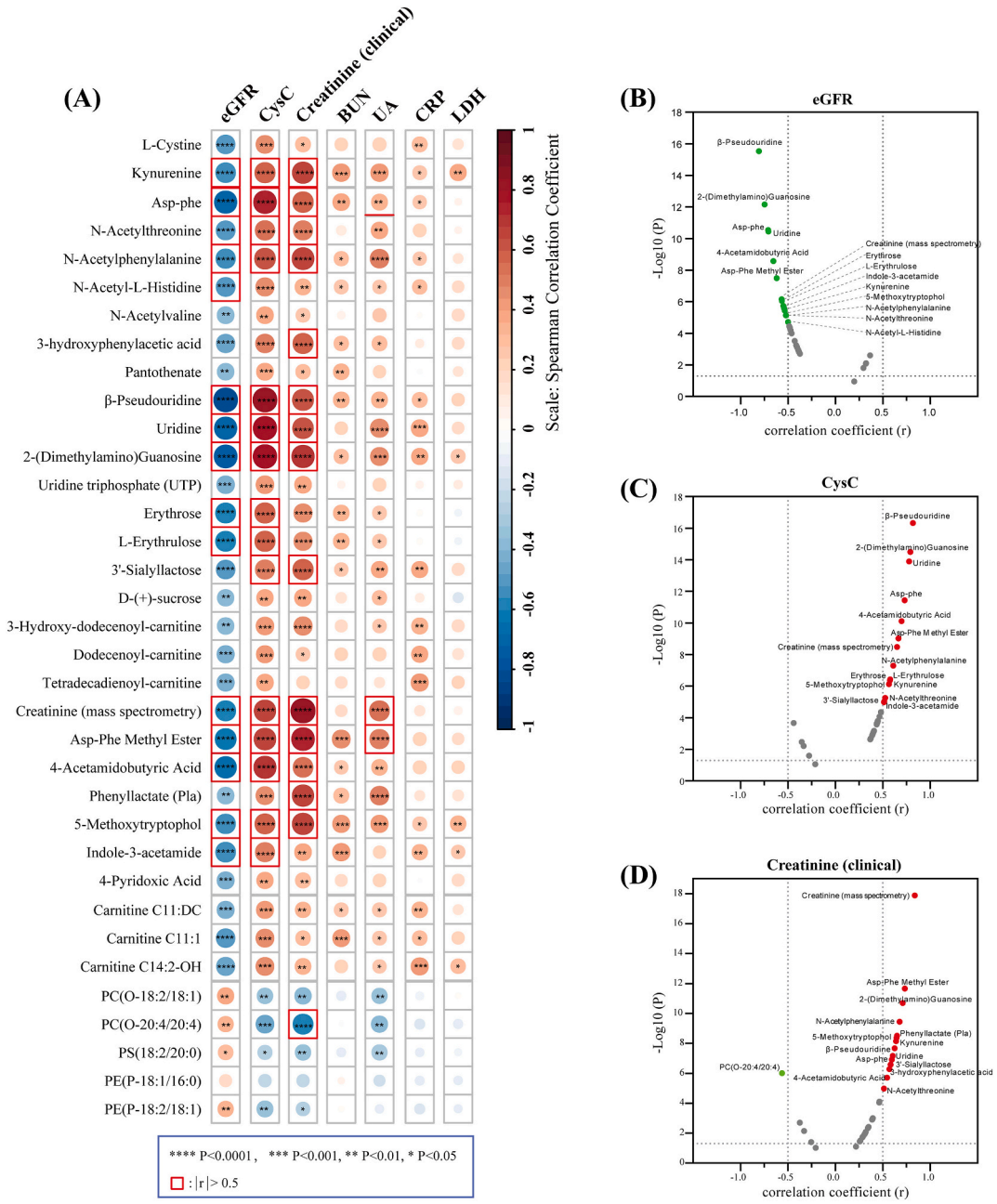

Fig. 4. Correlations between differential metabolites and typical clinical indicators.
(A) Correlation matrix illustrate spearman correlations between seven clinical indices and 35 differential metabolites ($P < 0.05$, FC > 1.2 or FC < 0.83, and VIP > 1) detected in the AAeGFR vs. NNeGFR and AAeGFR vs. NAeGFR groups. The order of the 35 metabolites is the same as that in Fig. 2C. Correlations with $p < 0.05$ are indicated with asterisks (p value: *, <0.05; **, <0.01; ***, <0.001; ****, <0.0001). Positive correlations are shown in red and negative correlations are shown in blue, with sizes and color intensity of circles representing the magnitude of the correlations. The red square frame represents Spearman correlation coefficient $|r| > 0.5$. (B–D) Scatter plots generated by −log(p) and correlation coefficient (r) shows the relationship between three clinical indicators (eGFR, Cys-c, and creatinine) and the 35 differential metabolites. The horizontal dashed line is the dividing line with a p value of 0.05, and the vertical dashed line is the dividing line with the correlation coefficient $|r| = 0.5$. Significantly changed metabolites ($p < 0.05$, $|r| > 0.5$) are marked in red (positive correlation) or green (negative correlation). (For interpretation of the references to color in this figure legend, the reader is referred to the web version of this article.)

in the body, which may be the reason for adverse kidney recovery. We speculate that the altered kynurenine pathway in tryptophan metabolism can cause a continuous decline in renal function, which in turn can promote the abnormal increase of kynurenine levels, thus forming a vicious circle. Eventually, this may lead to unfavorable kidney outcomes. Furthermore, Kyn/Tryp was also associated with a significantly higher incidence of CKD [36]. In our study, Kyn/Tryp was significantly higher in the AAeGFR group than in the NNeGFR or NAeGFR groups. Tryptophan metabolism and its major pathways, consisting of 5-hydroxytryptamine (also called serotonin), kynurenine, and aryl hydrocarbon receptor (AhR) pathways, play a central role in in the body's physiology and physiopathology [37]. Higher blood levels of tryptophan pathway metabolites were considered a consequence of lower eGFR [38]. The significant correlations (Fig. 4) between these typical metabolites and clinical renal function markers, including eGFR, Cys-c, and creatinine, further proved that metabolomics can help select metabolites to be clinically useful biomarkers.

Cysteine and methionine metabolism was also perturbed in the three

groups in our study. One important metabolite involved in this metabolic pathway is S-adenosylhomocysteine (SAH), which is strongly associated with the eGFR in a cardiovascular low-risk population [39]. A previous study showed that the level of SAH was significantly elevated in patients with high kidney disease severity [40]. Although the urea cycle is mainly expressed in the liver, urea plays an important role in the urine concentrating process in the kidney. Several metabolites in the urea cycle were upregulated in patients with abnormal eGFR in our study. Increased arginase activity has been reported to be tightly associated with the progression of diabetic nephropathy and hypertensive nephropathy to end-stage renal failure [41]. We have sufficient reason to believe that dysregulation of the above three metabolic pathways, given their prominence in our study, are caused by renal function decline in severely ill COVID-19 survivors. Moreover, persistent perturbation of these metabolic pathways can exacerbate renal function.

There are several limitations to our study. First, we used eGFR to represent kidney function instead of GFR, measured using the inulin clearance method. However, the latter is impractical for a large, general population-based study. Second, this study only focused on the recovery of renal function in severely ill COVID-19 survivors. Longitudinal changes in eGFR in patients with mild, moderate, and asymptomatic COVID-19 need to be confirmed in other studies. Third, the patients did not undergo urinalysis (proteinuria and hematuria); thus, urine metabolites were not measured or analyzed in the present study. Fourth, this study was largely limited by the small sample, and all patients were from China. Therefore, future studies should also include patients from other countries to more comprehensively understand post-hospital renal sequelae in COVID-19.

5. Conclusions

Our findings showed the changes in eGFR in severely ill COVID-19 survivors from hospitalization to 3 months after discharge and the metabolomic differences among patients with different eGFR change patterns. Pathway analysis revealed that tryptophan metabolism, cysteine and methionine metabolism, vitamin B6 metabolism, and urea cycle were four mainly perturbed metabolic pathways. Perturbation of these pathways is associated with abnormal renal function and is likely related to kidney sequelae caused by COVID-19. Altered concentrations of metabolites are the consequence of decreased eGFR, and these findings can nominate potential therapeutics to help recover the renal function of COVID-19 survivors.

Supplementary data to this article can be found online at https://doi.org/10.1016/j.bbadis.2021.166289.

CRediT authorship contribution statement

Mei Zhou: Conceptualization, Data curation, Formal analysis, Investigation, Methodology, Visualization, Writing – original draft, Writing – review & editing. **Xueyun Tan:** Conceptualization, Data curation, Investigation, Methodology, Visualization, Writing – original draft, Writing – review & editing. **Ping Luo:** Conceptualization, Data curation, Formal analysis, Investigation, Methodology, Visualization, Writing – original draft, Writing – review & editing. **Juanjuan Xu:** Conceptualization, Data curation, Investigation, Methodology, Resources, Writing – review & editing. **Zhengrong Yin:** Conceptualization, Data curation, Investigation, Methodology, Writing – review & editing. **Tingting Liao:** Conceptualization, Data curation, Investigation, Methodology, Writing – review & editing. **Sufei Wang:** Conceptualization, Data curation, Investigation, Methodology, Writing – review & editing. **Zhihui Wang:** Conceptualization, Data curation, Investigation, Methodology, Writing – review & editing. **Yang Jin:** Conceptualization, Funding acquisition, Methodology, Project administration, Resources, Supervision, Writing – review & editing.

Declaration of competing interest

The authors declare that they have no known competing financial interests or personal relationships that could have appeared to influence the work reported in this paper.

Acknowledgements

The authors would like to thank Dr. Huang Jing from the Department of Nephrology, Wuhan Union Hospital, for her help in the interpretation and analysis of renal function related data. In particular, we are grateful for the assistance provided by Dr. hui Zheng and Mr. Xi Zhan from the Wuhan Metware Biotechnology Co., Ltd. for their kind help on metabolomics analysis. The graphical abstract in this study was built through the website of BioRender.com.

Funding

This study was supported by the National Natural Science Special Foundation of China (82041018), Ministry of Science and Technology of the People's Republic of China (2020YFC0844300), and the Fundamental Research Funds for the Central Universities (HUST: 2020kfyXGYJ011). The research sponsors did not participate in the research design, data collection, analysis, and interpretation, nor did they participate in the writing of the manuscript and the decision to submit the manuscript for publication.

Data sharing

Anonymized clinical and metabolomic data are available on request, subject to an internal review by YJ and MZ to ensure that the participants' anonymity and confidentiality are protected, with completion of a data-sharing agreement, and in accordance with the Wuhan Union hospital's institutional review boards and institutional guidelines. Please submit requests for participant-related clinical and metabolomic data to YJ (whuhjy@126.com).

References

[1] World Health Organization, Coronavirus disease (COVID-19) dashboard. https://covid19.who.int (Accessed 21 March 2021).
[2] J.S. Hirsch, J.H. Ng, D.W. Ross, P. Sharma, H.H. Shah, R.L. Barnett, A.D. Hazzan, S. Fishbane, K.D. Jhaveri, Acute kidney injury in patients hospitalized with COVID-19, Kidney Int. 98 (2020) 209–218.
[3] L. Chan, K. Chaudhary, A. Saha, K. Chauhan, A. Vaid, S. Zhao, I. Paranjpe, S. Somani, F. Richter, R. Miotto, A. Lala, A. Kia, P. Timsina, L. Li, R. Freeman, R. Chen, J. Narula, A.C. Just, C. Horowitz, Z. Fayad, C. Cordon-Cardo, E. Schadt, M. A. Levin, D.L. Reich, V. Fuster, B. Murphy, J.C. He, A.W. Charney, E.P. Böttinger, B. S. Glicksberg, S.G. Coca, G.N. Nadkarni, AKI in hospitalized patients with COVID-19, J. Am. Soc. Nephrol. 32 (2021) 151–160.
[4] M. Fisher, J. Neugarten, E. Bellin, M. Yunes, L. Stahl, T.S. Johns, M.K. Abramowitz, R. Levy, N. Kumar, M.H. Mokrzycki, M. Coco, M. Dominguez, K. Prudhvi, L. Golestaneh, AKI in hospitalized patients with and without COVID-19: a comparison study, J. Am. Soc. Nephrol. 31 (2020) 2145–2157.
[5] Y. Cheng, R. Luo, K. Wang, M. Zhang, Z. Wang, L. Dong, J. Li, Y. Yao, S. Ge, G. Xu, Kidney disease is associated with in-hospital death of patients with COVID-19, Kidney Int. 97 (2020) 829–838.
[6] G. Pei, Z. Zhang, J. Peng, L. Liu, C. Zhang, C. Yu, Z. Ma, Y. Huang, W. Liu, Y. Yao, R. Zeng, G. Xu, Renal involvement and early prognosis in patients with COVID-19 pneumonia, J. Am. Soc. Nephrol. 31 (2020) 1157–1165.
[7] J. Nugent, A. Aklilu, Y. Yamamoto, M. Simonov, F. Li, A. Biswas, L. Ghazi, J. Greenberg, S. Mansour, D. Moledina, F.P. Wilson, Assessment of acute kidney injury and longitudinal kidney function after hospital discharge among patients with and without COVID-19, JAMA Netw. Open 4 (2021), e211095.
[8] S.M. Titan, G. Venturini, K. Padilha, G. Tavares, R. Zatz, I. Bensenor, P.A. Lotufo, E. P. Rhee, R.I. Thadhani, A.C. Pereira, Metabolites related to eGFR: evaluation of candidate molecules for GFR estimation using untargeted metabolomics, Clin. Chim. Acta Int. J. Clin. Chem. 489 (2019) 242–248.
[9] L.A. Inker, C.H. Schmid, H. Tighiouart, J.H. Eckfeldt, H.I. Feldman, T. Greene, J. W. Kusek, J. Manzi, F. Van Lente, Y.L. Zhang, J. Coresh, A.S. Levey, Estimating glomerular filtration rate from serum creatinine and cystatin C, N. Engl. J. Med. 367 (2012) 20–29.

[10] A.A. Shetty, I. Tawhari, L. Safar-Boueri, N. Seif, A. Alahmadi, R. Gargiulo, V. Aggarwal, I. Usman, S. Kisselev, A.G. Gharavi, Y. Kanwar, S.E. Quaggin, COVID-19-associated glomerular disease, J. Am. Soc. Nephrol. 32 (2021) 33–40.
[11] X. Nie, L. Qian, R. Sun, B. Huang, X. Dong, Q. Xiao, Q. Zhang, T. Lu, L. Yue, S. Chen, X. Li, Y. Sun, L. Li, L. Xu, Y. Li, M. Yang, Z. Xue, S. Liang, X. Ding, C. Yuan, L. Peng, W. Liu, X. Yi, M. Lyu, G. Xiao, X. Xu, W. Ge, J. He, J. Fan, J. Wu, M. Luo, X. Chang, H. Pan, X. Cai, J. Zhou, J. Yu, H. Gao, M. Xie, S. Wang, G. Ruan, H. Chen, H. Su, H. Mei, D. Luo, D. Zhao, F. Xu, Y. Li, Y. Zhu, J. Xia, Y. Hu, T. Guo, Multi-organ proteomic landscape of COVID-19 autopsies, Cell.
[12] J. Boelaert, F. Lynen, G. Glorieux, E. Schepers, N. Neirynck, R. Vanholder, Metabolic profiling of human plasma and urine in chronic kidney disease by hydrophilic interaction liquid chromatography coupled with time-of-flight mass spectrometry: a pilot study, Anal. Bioanal. Chem. 409 (2017) 2201–2211.
[13] M.E. Grams, A. Tin, C.M. Rebholz, T. Shafi, A. Köttgen, R.D. Perrone, M.J. Sarnak, L.A. Inker, A.S. Levey, J. Coresh, Metabolomic alterations associated with cause of CKD, Clin. J. Am. Soc. Nephrol. 12 (2017) 1787–1794.
[14] C. Huang, L. Huang, Y. Wang, X. Li, L. Ren, X. Gu, L. Kang, L. Guo, M. Liu, X. Zhou, J. Luo, Z. Huang, S. Tu, Y. Zhao, L. Chen, D. Xu, Y. Li, C. Li, L. Peng, Y. Li, W. Xie, D. Cui, L. Shang, G. Fan, J. Xu, G. Wang, Y. Wang, J. Zhong, C. Wang, J. Wang, D. Zhang, B. Cao, 6-Month consequences of COVID-19 in patients discharged from hospital: a cohort study, Lancet 397 (2021) 220–232.
[15] J. Xu, M. Zhou, P. Luo, Z. Yin, S. Wang, T. Liao, F. Yang, Z. Wang, D. Yang, Y. Peng, W. Geng, Y. Li, H. Zhang, J. Yang, Plasma metabolomic profiling of patients recovered from COVID-19 with pulmonary sequelae 3 months after discharge, Clin. Infect. Dis. (2021), https://doi.org/10.1093/cid/ciab147. PMID: 33596592.
[16] World Health Organization, COVID-19 clinical management: living guidance, 25 January 2021. https://www.who.int/publications/i/item/WHO-2019-nCoV-clinical-2021-1. Accessed.
[17] D. Wu, T. Shu, X. Yang, J.-X. Song, M. Zhang, C. Yao, W. Liu, M. Huang, Y. Yu, Q. Yang, T. Zhu, J. Xu, J. Mu, Y. Wang, H. Wang, T. Tang, Y. Ren, Y. Wu, S.-H. Lin, Y. Qiu, D.-Y. Zhang, Y. Shang, X. Zhou, Plasma metabolomic and lipidomic alterations associated with COVID-19, Natl. Sci. Rev. 7 (2020) 1157–1168.
[18] D.Q. Chen, G. Cao, H. Chen, D. Liu, W. Su, X.Y. Yu, N.D. Vaziri, X.H. Liu, X. Bai, L. Zhang, Y.Y. Zhao, Gene and protein expressions and metabolomics exhibit activated redox signaling and wnt/β-catenin pathway are associated with metabolite dysfunction in patients with chronic kidney disease, Redox Biol. 12 (2017) 505–521.
[19] Y. Zuo, S.K. Estes, R.A. Ali, A.A. Gandhi, S. Yalavarthi, H. Shi, G. Sule, K. Gockman, J.A. Madison, M. Zuo, V. Yadav, J. Wang, W. Woodard, S.P. Lezak, N.L. Lugogo, S. A. Smith, J.H. Morrissey, Y. Kanthi, J.S. Knight, Prothrombotic autoantibodies in serum from patients hospitalized with COVID-19, Sci. Transl. Med. 12 (2020).
[20] H. Su, M. Yang, C. Wan, L.X. Yi, F. Tang, H.Y. Zhu, F. Yi, H.C. Yang, A.B. Fogo, X. Nie, C. Zhang, Renal histopathological analysis of 26 postmortem findings of patients with COVID-19 in China, Kidney Int. 98 (2020) 219–227.
[21] D.P. Basile, Rarefaction of peritubular capillaries following ischemic acute renal failure: a potential factor predisposing to progressive nephropathy, Curr. Opin. Nephrol. Hypertens. 13 (2004) 1–7.
[22] L.S. Chawla, P.W. Eggers, R.A. Star, P.L. Kimmel, Acute kidney injury and chronic kidney disease as interconnected syndromes, N. Engl. J. Med. 371 (2014) 58–66.
[23] P. Sekula, O.N. Goek, L. Quaye, C. Barrios, A.S. Levey, W. Römisch-Margl, C. Menni, I. Yet, C. Gieger, L.A. Inker, J. Adamski, W. Gronwald, T. Illig, K. Dettmer, J. Krumsiek, P.J. Oefner, A.M. Valdes, C. Meisinger, J. Coresh, T. D. Spector, R.P. Mohney, K. Suhre, G. Kastenmüller, A. Köttgen, A metabolome-wide association study of kidney function and disease in the general population, J. Am. Soc. Nephrol. 27 (2016) 1175–1188.
[24] B. Hocher, J. Adamski, Metabolomics for clinical use and research in chronic kidney disease, Nat. Rev. Nephrol. 13 (2017) 269–284.
[25] Y. Zhang, S. Guo, C. Xie, J. Fang, Uridine metabolism and its role in glucose, lipid, and amino acid homeostasis, Biomed. Res. Int. 2020 (2020), 7091718.
[26] T. Niwa, N. Takeda, H. Yoshizumi, RNA metabolism in uremic patients: accumulation of modified ribonucleosides in uremic serum. Technical note, Kidney Int. 53 (1998) 1801–1806.
[27] S.P. Coburn, R.D. Reynolds, J.D. Mahuren, W.E. Schaltenbrand, Y. Wang, K. L. Ericson, M.P. Whyte, Y.M. Zubovic, P.J. Ziegler, D.L. Costill, W.J. Fink, D. R. Pearson, T.A. Pauly, K.G. Thampy, J. Wortsman, Elevated plasma 4-pyridoxic acid in renal insufficiency, Am. J. Clin. Nutr. 75 (2002) 57–64.
[28] S. Debnath, C. Velagapudi, L. Redus, F. Thameem, B. Kasinath, C.E. Hura, C. Lorenzo, H.E. Abboud, J.C. O'Connor, Tryptophan metabolism in patients with chronic kidney disease secondary to type 2 diabetes: relationship to inflammatory markers, Int. J. Tryptophan Res. 10 (2017) (1178646917694600).
[29] J.R. Liu, H. Miao, D.Q. Deng, N.D. Vaziri, P. Li, Y.Y. Zhao, Gut microbiota-derived tryptophan metabolism mediates renal fibrosis by aryl hydrocarbon receptor signaling activation, Cell. Mol. Life Sci. 78 (2021) 909–922.
[30] D. Changsirivathanathamrong, Y. Wang, D. Rajbhandari, G.J. Maghzal, W.M. Mak, C. Woolfe, J. Duflou, V. Gebski, C.G. dos Remedios, D.S. Celermajer, R. Stocker, Tryptophan metabolism to kynurenine is a potential novel contributor to hypotension in human sepsis, Crit. Care Med. 39 (2011) 2678–2683.
[31] E.R. Pedersen, G.F. Svingen, H. Schartum-Hansen, P.M. Ueland, M. Ebbing, J. E. Nordrehaug, J. Igland, R. Seifert, R.M. Nilsen, O. Nygård, Urinary excretion of kynurenine and tryptophan, cardiovascular events, and mortality after elective coronary angiography, Eur. Heart J. 34 (2013) 2689–2696.
[32] Y. Wang, H. Liu, G. McKenzie, P.K. Witting, J.P. Stasch, M. Hahn, D. Changsirivathanathamrong, B.J. Wu, H.J. Ball, S.R. Thomas, V. Kapoor, D. S. Celermajer, A.L. Mellor, J.F. Keaney Jr., N.H. Hunt, R. Stocker, Kynurenine is an endothelium-derived relaxing factor produced during inflammation, Nat. Med. 16 (2010) 279–285.
[33] R.E. Silva, J.L. Baldim, D.A. Chagas-Paula, M.G. Soares, J.H.G. Lago, R. V. Gonçalves, R.D. Novaes, Predictive metabolomic signatures of end-stage renal disease: a multivariate analysis of population-based data, Biochimie 152 (2018) 14–30.
[34] T. Thomas, D. Stefanoni, J.A. Reisz, T. Nemkov, L. Bertolone, R.O. Francis, K. E. Hudson, J.C. Zimring, K.C. Hansen, E.A. Hod, S.L. Spitalnik, A. D'Alessandro, COVID-19 infection alters kynurenine and fatty acid metabolism, correlating with IL-6 levels and renal status, JCI Insight 5 (2020).
[35] M.E. Collier, S. Zhang, N.S. Scrutton, F. Giorgini, Inflammation control and improvement of cognitive function in COVID-19 infections: is there a role for kynurenine 3-monooxygenase inhibition? Drug Discov. Today 26 (2021) 1473–1481.
[36] O.N. Goek, C. Prehn, P. Sekula, W. Römisch-Margl, A. Döring, C. Gieger, M. Heier, W. Koenig, R. Wang-Sattler, T. Illig, K. Suhre, J. Adamski, A. Köttgen, C. Meisinger, Metabolites associate with kidney function decline and incident chronic kidney disease in the general population, Nephrol. Dial. Transplant. 28 (2013) 2131–2138.
[37] A. Agus, J. Planchais, H. Sokol, Gut microbiota regulation of tryptophan metabolism in health and disease, Cell Host Microbe 23 (2018) 716–724.
[38] Y. Cheng, Y. Li, P. Benkowitz, C. Lamina, A. Köttgen, P. Sekula, The relationship between blood metabolites of the tryptophan pathway and kidney function: a bidirectional Mendelian randomization analysis, Sci. Rep. 10 (2020) 12675.
[39] A.M. Zawada, K.S. Rogacev, B. Hummel, J.T. Berg, A. Friedrich, H.J. Roth, R. Obeid, J. Geisel, D. Fliser, G.H. Heine, S-adenosylhomocysteine is associated with subclinical atherosclerosis and renal function in a cardiovascular low-risk population, Atherosclerosis 234 (2014) 17–22.
[40] A.L. Mindikoglu, A.R. Opekun, N. Putluri, S. Devaraj, D. Sheikh-Hamad, J. M. Vierling, J.A. Goss, A. Rana, G.K. Sood, P.K. Jalal, L.A. Inker, R.P. Mohney, H. Tighiouart, R.H. Christenson, T.C. Dowling, M.R. Weir, S.L. Seliger, W. R. Hutson, C.D. Howell, J.P. Raufman, L.S. Magder, C. Coarfa, Unique metabolomic signature associated with hepatorenal dysfunction and mortality in cirrhosis, Transl. Res. 195 (2018) 25–47.
[41] R.W. Caldwell, P.C. Rodriguez, H.A. Toque, S.P. Narayanan, R.B. Caldwell, Arginase: a multifaceted enzyme important in health and disease, Physiol. Rev. 98 (2018) 641–665.